

Evidence for pseudogap and phase-coherence gap separation by Andreev reflection experiments in $\text{Au}/\text{La}_{2-x}\text{Sr}_x\text{CuO}_4$ point-contact junctions

R.S. Gonnelli,* A. Calzolari, D. Daghero, L. Natale, and G.A. Ummarino
INFM - Dipartimento di Fisica, Politecnico di Torino, 10129 Torino, Italy

V.A. Stepanov
P.N. Lebedev Physical Institute, Russian Academy of Sciences, Moscow, Russia

M. Ferretti
Dipartimento di Chimica e Chimica Industriale, Università di Genova, 16146 Genova, Italy
 (Dated: December 6, 2018)

We present new $\text{Au}/\text{La}_{2-x}\text{Sr}_x\text{CuO}_4$ (LSCO) point-contact conductance measures as a function of voltage and temperature in samples with $0.08 \leq x \leq 0.2$. Andreev reflection features disappear at about the bulk T_c , giving no evidence of gap for $T > T_c$. The fit of the normalized conductance at any $T < T_c$ supports a $(s + d)$ -wave symmetry of the gap, whose dominant low- T s component follows the $T_c(x)$ curve in contrast with recent angle-resolved photoemission spectroscopy and quasi-particle tunneling data. These results prove the separation between pseudogap and phase-coherence superconducting gap in LSCO at $x \lesssim 0.2$.

PACS numbers: 74.50.+r, 74.25.Dw, 74.72.Dn

In a recent paper, G. Deutscher claimed the existence of two distinct energy scales - that is, two distinct gaps - in high- T_c superconductors (HTS) [1]. According to his discussion, one of these gaps should appear at $T^* > T_c$ in optimally-doped and underdoped samples and could be due to an incoherent pairing between charge carriers (whose physical origin is still under discussion) which leads to a pair pre-formation. This gap, Δ_p , would coincide with the pseudogap observed by angle-resolved photoemission spectroscopy (ARPES) and tunneling experiments. The second gap, Δ_c , would appear at T_c and would be associated to the achievement of the phase coherence by the pre-formed pairs and, consequently, to the onset of superconductivity. This *phase-coherence* gap can be observed only by experimental tools sensitive to the phase coherence of the pairs, i.e. Josephson effect and/or Andreev reflection experiments. At the present moment low-temperature tunneling [2] and very recent ARPES experiments [3] in $\text{La}_{2-x}\text{Sr}_x\text{CuO}_4$ (LSCO) have shown at $x < 0.2$ the presence of a large gap which increases at the lowering of the doping level. Very few experiments have instead been performed to investigate the Andreev gap [4, 5], and, to our knowledge, none at all to study in detail its dependence on the temperature and on the doping in the region from overdoped to underdoped.

In this letter, we present and discuss the results of point-contact experiments on $\text{La}_{2-x}\text{Sr}_x\text{CuO}_4$ samples. Despite the polycrystalline nature of the samples, a very careful point-contact technique allowed obtaining, for the first time, very good Andreev reflection curves in a broad temperature and doping range. In order to extract information about the dependence of the Andreev gap on x

and T , we fitted the experimental curves with the generalized BTK model by Y. Tanaka and S. Kashiwaya [6] for various possible symmetries of the order parameter. We found that the dependence of the Andreev gap on temperature and Sr content experimentally proves the existence of two distinct energy scales, a large pseudogap and a smaller superconducting gap, in LSCO.

The high-quality $\text{La}_{2-x}\text{Sr}_x\text{CuO}_4$ polycrystalline samples used for our measurements were prepared by conventional solid-state reaction at 1000°C by using stoichiometric amounts of the high-purity precursor oxides La_2O_3 , CuO , and SrO_2 . After the first reaction step the bulk materials were finely ground, pressed into small rectangular bars and sintered to obtain higher density samples. The sintering temperature was selected between 1100 and 1150°C for different Sr amount. When the dopant concentration was greater than $x=0.1$, quenching was required from higher temperatures (1170°C) to ensure chemical homogeneity. All samples were structurally characterized by XRD powder diffraction [7], and their actual stoichiometry was determined by means of EDS microprobe analysis, which evidenced the absence of impurities and confirmed their nominal Sr concentrations: $x = 0.08, 0.10, 0.12, 0.13, 0.15$ and 0.20 . The typical linear dimension of the grains, as observed by means of AFM or SEM measurements, was $5 \div 10 \mu\text{m}$. AC susceptibility and resistivity measurements were used to determine the critical temperatures, which were in good agreement with the standard curve of T_c as a function of x for LSCO [8]. The width of the resistive transition was of the order of $3 \div 5$ K for all the Sr contents.

We performed on these samples point-contact experiments by using very sharp Au tips, whose ending-part diameter was always less than $\sim 2 \mu\text{m}$ [9], obtained by electro-chemical etching (with a $\text{HNO}_3 + \text{HCl}$ solution) of a 0.2 mm diameter Au wire. The rather large dimen-

*Corresponding author. E-mail:gonnelli@polito.it

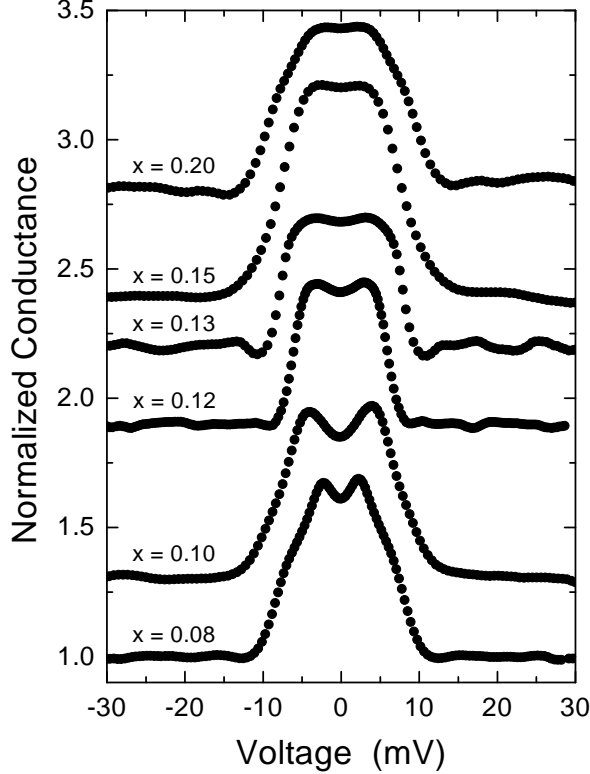


FIG. 1: The normalized conductances of Au/LSCO point-contact junctions for various doping levels ($0.08 \leq x \leq 0.2$) and at low temperature ($4.22 \text{ K} \leq T \leq 5.61 \text{ K}$). The curves are vertically displaced for clarity.

sions of the LSCO grains and the sharpness of the tips allowed us to obtain very often single-grain touches and, therefore, good SN junctions with very good Andreev reflection characteristics. Due to the stability of the point contact, whose resistance was in the range $1 \div 3 \Omega$ for all the samples, we were able to follow the evolution of the conductance curves on heating the junction from 4.2 K up to the temperature T_c^A at which the dynamic conductance dI/dV was flat.

Figure 1 shows the low-temperature experimental *normalized* conductance data (vertically shifted for clarity) for the six doping values previously mentioned. We systematically normalized only the data sets for which dI/dV at $|V| > 20 \text{ mV}$ was reasonably constant and did not show sensible variations at the change of temperature. This last condition simply corresponds to the request of contact stability during the temperature scan up to T_c^A . All the results that we show in the present letter are obtained from this kind of data.

The experimental data of Fig. 1 are examples of the high-quality Andreev reflection curves we obtained. Their shape and height are in most cases close to the ideal ones predicted for a very low potential barrier by the well-known BTK model [10]. However, some differences are present. First, the maximum value is less than

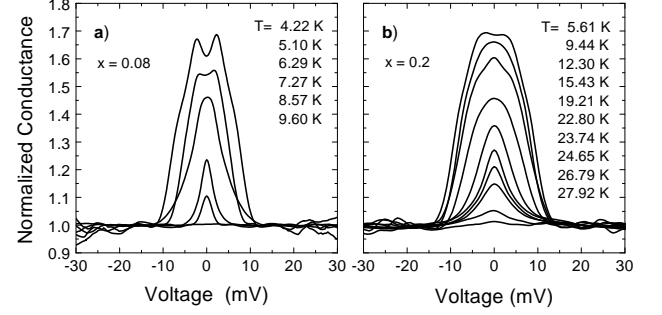


FIG. 2: Temperature dependence of the normalized Andreev conductance in LSCO samples with $x = 0.08$ (a) and 0.2 (b).

that expected and the shape is not always compatible with a pure *s*-wave symmetry of the order parameter. Moreover, some more or less pronounced oscillations of dI/dV are present at $|V| \gtrsim 10 \text{ mV}$. These oscillations have been already observed in high- T_c superconductors and can be due to the presence of localized electron states in the interface potential barrier [11].

Figure 2 shows the temperature dependence of the normalized conductance in samples with $x=0.08$ (a) and 0.2 (b). As it happens in all the other samples, the Andreev features disappear at the bulk T_c (or at a slightly lower temperature) and a change in the shape of the curves is evident at the increase of T (see, for example, the curve at $T=12.3 \text{ K}$ in Fig. 2b). As we will show later, this last feature can be explained by a change in the relative weight of the isotropic and anisotropic gap components.

To evaluate the gap and to study its dependence on the doping content, we fitted the normalized conductance curves by using the generalized BTK model introduced few years ago by S. Kashiwaya and Y. Tanaka [6]. In order to properly fit our data in the whole temperature range, we introduced in the original model of Ref. [6] the effect of the temperature and of the broadening parameter Γ which takes into account the finite lifetime of the quasiparticles. Various symmetries of the order parameter were used (*s*, *s*+*id*, *s*+*d* and anisotropic *s*). The pure $d_{x^2-y^2}$ symmetry was not considered because it was unable to properly fit the low-voltage part of all our data for any value of the fit parameters.

In the case of mixed pair symmetry and at constant T the free parameters of the fit are: the values of the isotropic and anisotropic components of the gap (Δ_{is} and Δ_{an}), the parameter Z (proportional to the potential barrier height), the lifetime broadening Γ and the angle α between the *a* axis and the normal to the S-N interface [6]. Actually, when $Z \leq 0.3$ (as in our case) the choice of α has a negligible influence on the values of Δ_{is} and Δ_{an} determined by the fit, independently of the symmetry used. Therefore, α is *not* a critical parameter and thus we put $\alpha = 0$ in all cases. Z was determined by the fits in the various symmetries of the lowest-temperature

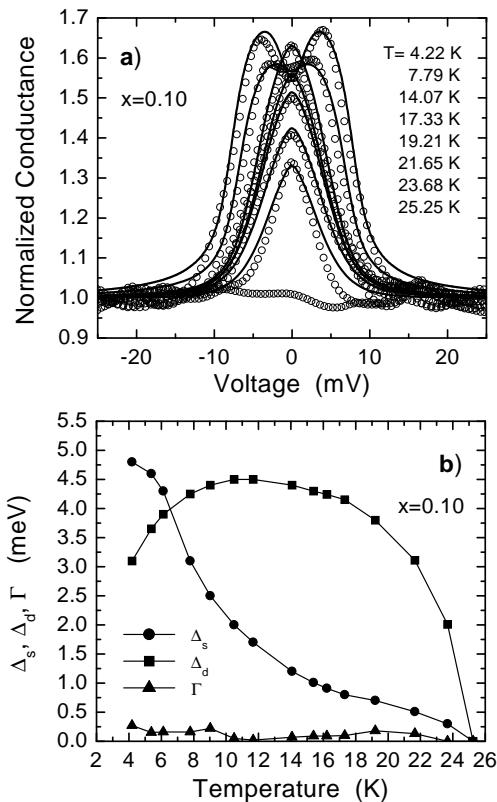


FIG. 3: (a) Normalized conductance curves at various temperatures up to T_c^A in LSCO with $x = 0.1$ and best fit curves in $s+d$ symmetry; (b) Temperature dependencies of the s and d gap components and of the lifetime parameter determined by the fits of Fig. 3a.

curves and, due to the stability of the contact resistances, was supposed to remain constant at the increase of the temperature. The parameters Δ_{is} , Δ_{an} and Γ were varied in order to fit the data, but always keeping Γ as small as possible.

The theoretical conductance curves which best fit the low-temperature experimental data of Fig. 1 are those calculated in the $(s+d)$ - or in the pure s -wave symmetry, depending on the Sr content. In all cases, the s -wave component is dominant. It is very important to notice that the value of the isotropic component of the gap is actually *almost independent* of the particular symmetry used for the fit, and therefore can be considered a very robust parameter.

A good fit of the conductance curves *in the whole temperature range* can be obtained only by using the $(s+d)$ -wave symmetry with suitable (and T -dependent) weights for the s and d components. Figure 3a shows an example of the temperature dependence of the normalized conductance in a sample with $x = 0.1$ (open symbols) and the corresponding $(s+d)$ -wave best-fit curves (solid lines). For clarity, only few of the measured curves are shown. The fits are good up to the critical temperature of the junction ($T_c^A \approx 25.3$ K) at which the Andreev fea-

tures disappear. Similar results (always in $(s+d)$ -wave symmetry) have been obtained in all the other LSCO samples. Incidentally, Figure 3b reports the temperature dependence of the s and d components of the gap in LSCO with $x = 0.1$ determined by the fits of Fig. 3a. It is clear that the temperature dependence of the two components is quite different. The shape of the $\Delta_s(T)$ curve (and of the $\Delta_d(T)$ one when the d component is present) is common to all the doping contents. However, in the underdoped and optimally-doped samples Δ_d is smaller than Δ_s at low T and becomes dominant at higher temperature, while in the overdoped ones ($x = 0.2$) Δ_d never exceeds Δ_s . Further details are presented elsewhere [12].

Let us now go back to the discussion of the low-temperature conductance curves shown in Fig. 1. The results of their fits are consistent with those obtained in LSCO by Deutscher *et al.* [4]. Table I shows the temperature of the junction and the values of Δ_s , Δ_d , Γ and Z for the curves of Fig. 1 together with the Andreev critical temperature T_c^A and $2\Delta_s/k_B T_c^A$ for every doping value.

Doping	T (K)	Δ_s (meV)	Δ_d (meV)	Γ (meV)	Z	T_c^A (K)	$2\Delta_s/k_B T_c^A$
0.08	4.22	3.4	2.5	0.19	0.20	9.6	8.2
0.10	4.22	4.8	3.1	0.27	0.23	25.3	4.4
0.12	4.22	5.6	0	0.92	0.18	26.0	5.0
0.13	4.22	6.8	0	1.50	0.17	29.1	5.4
0.15	4.65	6.8	0	0.44	0.08	35.3	4.5
0.20	5.61	6.0	3.5	1.00	0.13	27.9	5.0

TABLE I: Best-fit parameters and temperatures for the curves of Fig. 1

In Fig. 4 the doping dependencies of the *low-temperature* Δ_s and Δ_d (solid circles and solid squares, respectively) determined from the data of Fig. 1 are compared to those of the ARPES leading-edge shift (LE) recently determined in LSCO [3] (open circles) and of the gap determined by tunneling measurements (open squares)[2]. Both the ARPES LE and the tunneling gap values increase monotonically at the decrease of the doping and reach very large values ($15 \div 20$ meV for the ARPES LE in strongly underdoped samples). On the contrary, the dominant isotropic gap component determined from Andreev reflection data increases at the decrease of the doping in the overdoped region up to a maximum approximately located at the optimum doping, and then strongly reduces in the underdoped region, following the critical temperature behaviour (thick solid line). Let us stress that this conclusion *does not* depend on the model used to fit the experimental data, and holds true even if the Andreev gap is simply identified with the energy at which the conductance at negative (positive) bias has the maximum (minimum) slope.

The main findings that follow from the results shown above can be so summarized: i) all the Andreev reflection

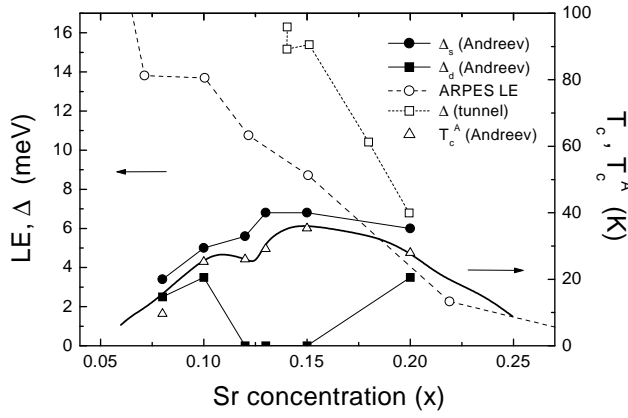


FIG. 4: Doping dependence of the ARPES leading-edge shift (open circles, from Ref.[3]), of the tunneling gap (open squares, from Ref.[2]) and of our point-contact Andreev gap (solid circles for Δ_s and solid squares for Δ_d) in LSCO. The temperatures T_c^A at which the Andreev features disappear in our samples are also reported (up triangles) and compared to the T_c vs x curve from Ref.[8] (thick line).

features disappear at about the bulk T_c of the samples (see Fig. 4, open triangles). The Andreev spectroscopy thus gives no evidence of gap at $T > T_c$ in LSCO, even in the underdoped region; ii) the fit of the Andreev curves for all x values indicate that, at *low-temperature*, the *s*-wave component of the gap is dominant and independent of the symmetry used for the fit. Pure *d*-wave symmetry is unable to fit the data; iii) in contrast with the ARPES leading-edge shift [3] and the gap determined by tunneling [2], the low-temperature dominant Andreev Δ_s decreases at the decrease of x in the underdoped region and globally follows the T_c vs x behaviour.

These results give a complete experimental evidence for the existence of two energy scales in LSCO. The smallest one represents the phase-coherence (superconducting) gap, while the greatest is related to the gap-like features (pseudogap) observed by ARPES and quasiparticle tun-

neling experiments. As shown in Fig. 4, these two energy scales seem to merge slightly above the optimum doping. The present results are also a direct prove that the pseudogap is a property of the non-superconducting state of LSCO. The question arises of what could be its origin. Despite the large number of theoretical models proposed, the answer is still not clear.

Very recently, a two-gap model appeared in literature [13] which explains the pseudogap features in underdoped cuprate superconductors in the framework of incoherent pre-formed pairs around the M points of the Brillouin zone. According to this model, a bifurcation at $x_b > x_{opt}$ is expected between the mean-field T_c curve (which has a maximum at $x = x_{opt}$) and the temperature of pair pre-formation T^* (assumed to be linearly increasing at the lowering of x). Another recent model [14], on the contrary, analyzes the transition to the superconducting state in the presence of a preformed normal-state pseudogap resulting from interactions in the particle-hole channel, and predicts for the superconducting gap and the ARPES leading-edge shift the same doping dependence as T_c and T^* respectively, in very good agreement with our experimental results. In conclusion, both these approaches seem able to explain the experimental findings shown in Fig. 4.

Although further theoretical investigation is necessary to enlighten the real nature of the pseudogap state, we believe to have experimentally proved in a broad doping range ($0.08 \leq x \leq 0.2$) the existence of two energy scales in LSCO, related to the separation between a large incoherent pseudogap and a smaller phase-coherent superconducting gap which follows the T_c vs. x behaviour.

The interpretation of these results could play an essential role in the way to the comprehension of the microscopic mechanism leading to high- T_c superconductivity in LSCO.

Many thanks are due to G. Deutscher and A. Perali for useful discussions. This work has been done under the Advanced Research Project "PRA-SPIS" of the Istituto Nazionale di Fisica della Materia (INFM).

-
- [1] G. Deutscher, Nature 397 (1999) 410.
 - [2] T. Nakano *et al.*, J. Phys. Soc. Jpn. **67**, 2622 (1998); M. Oda *et al.*, Physica C **341-348**, 847 (2000).
 - [3] A. Ino *et al.*, cond-mat/0005370, May 2000.
 - [4] N.S. Achsraf *et al.*, J. Low Temp. Phys. **105**, 329 (1996); G. Deutscher *et al.*, Physica C **282-287**, 140 (1997).
 - [5] Y. Dagan, A. Kohen and G. Deutscher, Phys. Rev. B **61**, 7012 (2000).
 - [6] Y. Tanaka and S. Kashiwaya, Phys. Rev. Lett. **74**, 3451 (1995); S. Kashiwaya *et al.*, Phys. Rev. B **53**, 2267 (1996); S. Kashiwaya and Y. Tanaka, Rep. Prog. Phys. **63** 1641 (2000).
 - [7] M. Napoletano *et al.*, Physica C **319**, 229 (1999).
 - [8] Takagi *et al.*, Phys. Rev. B **40**, 2254 (1989).
 - [9] R.S. Gonnelli *et al.*, Int. J. Mod. Phys. B, in press.
 - [10] G.E. Blonder, M. Tinkham and T.M. Klapwijk, Phys. Rev. B **25**, 4515 (1982).
 - [11] V.A. Khlus, A.V. Dyomin, A.L.Zazunov, Physica C **214**, 413 (1993).
 - [12] R.S. Gonnelli *et al.*, to be published.
 - [13] A. Perali *et al.*, Phys. Rev. B. **62**, R9295 (2000).
 - [14] L. Benfatto, S. Caprara and C. Di Castro, Eur. Phys. J. B **17**, 95 (2000).